Supporting Information

Quantum Well Thickness Control of Hybrid Perovskite to Achieve Tunable Anisotropic Photoresponse

*Cheng-Dong Liu,‡ Chang-Chun Fan,‡ Bei-Dou Liang, Wei Wang, Ming-Liang Jin, Chang-Qing Jing, Jing-Meng Zhang, and Wen Zhang**

Jiangsu Key Laboratory for Science and Applications of Molecular Ferroelectrics and School of Chemistry and Chemical Engineering, Southeast University, Nanjing 211189, China.

E-mail: zhangwen@seu.edu.cn

Experimental Section

Materials and general characterizations.

2-Thiophenemethylamine (2TMA, 99%), lead acetate ($Pb(Ac)_2$, 99.9%), hydroiodic acid (HI, 48 *wt.*% in H_2O), Methylamine hydrochloride (MACl, 99.9%) and hypophosphorous acid (H_3PO_2 48 *wt.*% in H_2O) were commercially available and used as received without further purification.

Powder X-ray diffraction (PXRD) patterns were obtained on a Rigaku SmartLab X-ray diffraction instrument. Ultraviolet-visible (UV-vis) absorption spectra were measured with Shimadzu UV-2600 equipped with ISR-2600Plus integrating sphere. The single crystal growth was carried out using a home-made hydrothermal growth system.

Materials Synthesis.

The 2TM-n single crystal was synthesized in the concentrated HI solution, containing fixed 2TMA, and the stoichiometric ratio of $Pb(Ac)_2$ and MACl with an increasing number of layers. The resulting solution was cooled down gradually to 370 K to obtain a saturated solution. Then it was cooled down to 273 K at the rate of 20 K/day, resulting in tiny single crystals. By changing the cooling rate to 2 K/day, the large block crystals can be obtained.

Table S1. Reagent quantities used for 2TM-n single-crystal synthesis.

	2TM-1	2TM-2	2TM-3
$Pb(Ac)_2$	5 mmol	10 mmol	10 mmol
HI	30 mL	30 mL	30 mL
H_3PO_2	3 mL	3 mL	3 mL
MACl	/	5 mmol	7.5 mmol
2TMA	10 mmol	5 mmol	2.5 mmol

Device fabrication. The single-crystal device for photodetection was made by coating silver conducting paste on the crystal surface.

***I-V* measurement.** The photocurrent was measured by FS380 (Primarius). The LEDs were obtained from Thorlabs. The polarizer (Glan-Taylor prism) converts the LED laser beam into polarized light, and the polarization angle of the polarized light is then adjusted by a half-wave plate.

Theoretical calculations. DFT calculations were conducted by using VASP. Projector augmented wave method was adopted to define the ion-electron interactions. The exchange-correlation interaction was expressed by the PBE functional within the generalized gradient approximation. Grimme's dispersion-corrected semi-empirical DFT-D3 method was employed to evaluate van der Waals interactions. Energy cutoff of 500 eV and a 2×2×4 Monkhorst-Pack grid of k-points were used. VASPKIT was employed to perform post-processing analysis.[1]

Note S1.

The optical and electric anisotropy caused by the distinct charge density distribution of 2TM-n can be explained from the Fermi Golden Rule. We can get the electric dipole transition probability R for photon absorption per unit time:

$$R = \left(\frac{2\pi}{\hbar}\right)\sum_{k_c,k_v} |\langle c \,|\, H_{eR} \,|\, v\rangle|^2 \delta\left(E_c(k_c) - E_v(k) - \hbar\omega\right)$$

The $|v\rangle$ represents valence band state with energy E_v and wavevector k_v and the $|c\rangle$ represents conduction band state with energy E_c and wavevector k_c. The matrix element $|\langle c \,|\, H_{eR} \,|\, v\rangle|^2$ can be calculated as $|\langle c \,|\, H_{eR} \,|\, v\rangle|^2 = \left(\frac{e}{mc}\right)^2 |\langle c \,|\, A \cdot P \,|\, v\rangle|^2$, where $\boldsymbol{P}$ is the momentum operator and $\boldsymbol{A}$ is a vector potential. The amplitude of $\boldsymbol{A}$ can be written as $A = -\frac{E}{2q}\{exp[i(q \cdot r - \omega t)] + c.c.\}$, where *c.c.* stands for complex conjugate. The charge density distribution in the in-plane and out-of-plane direction is obviously different, which causes $|\langle c \,|\, H_{eR} \,|\, v\rangle|$ to have different integral values in the two directions. This also eventually results in different R for photon absorption per unit time in both the in-plane and out-of-plane direction, which demonstrates that the anisotropic polarized absorption of 2TM-n dominantly originates from the structural anisotropy.[2]

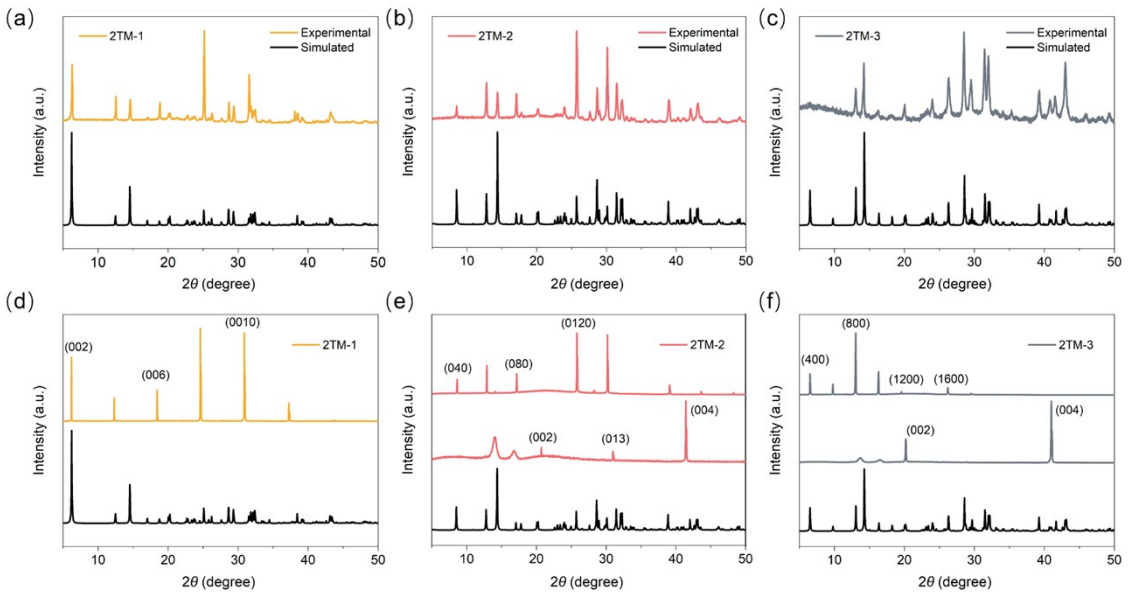

Fig. S1. PXRD patterns of (a, d) 2TM-1, (b, e) 2TM-2 and (c, f) 2TM-3.

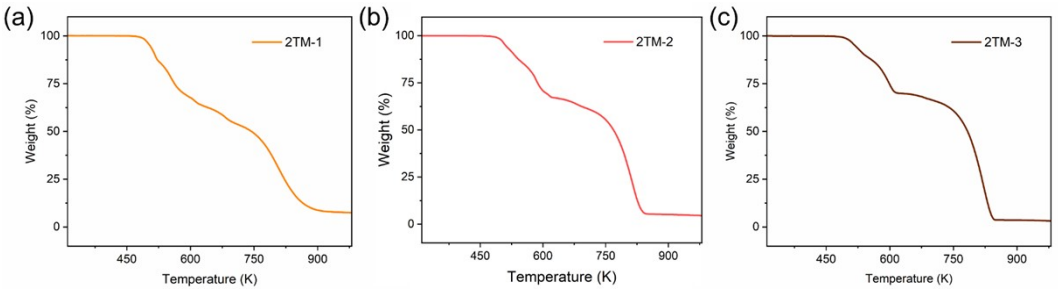

Fig. S2. Thermogravimetric analysis of (a) 2TM-1, (b) 2TM-2 and (c) 2TM-3.

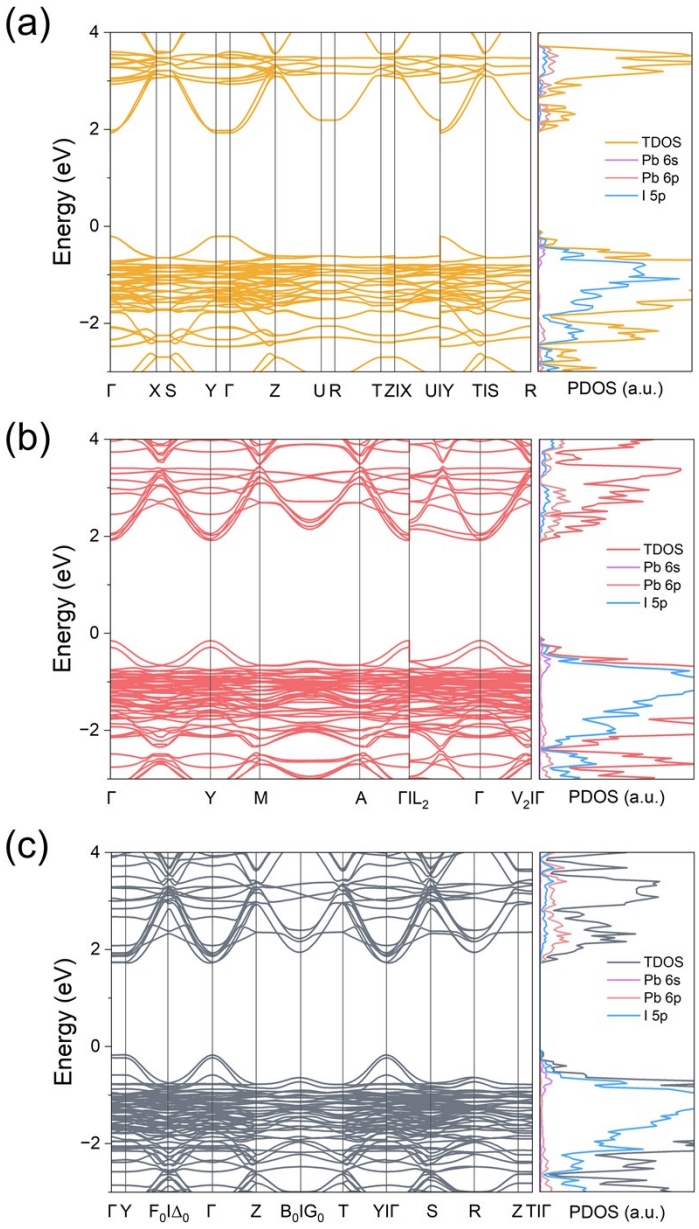

Fig. S3. Calculated band structures of (a) 2TM-1, (b) 2TM-2, and (c) 2TM-3.

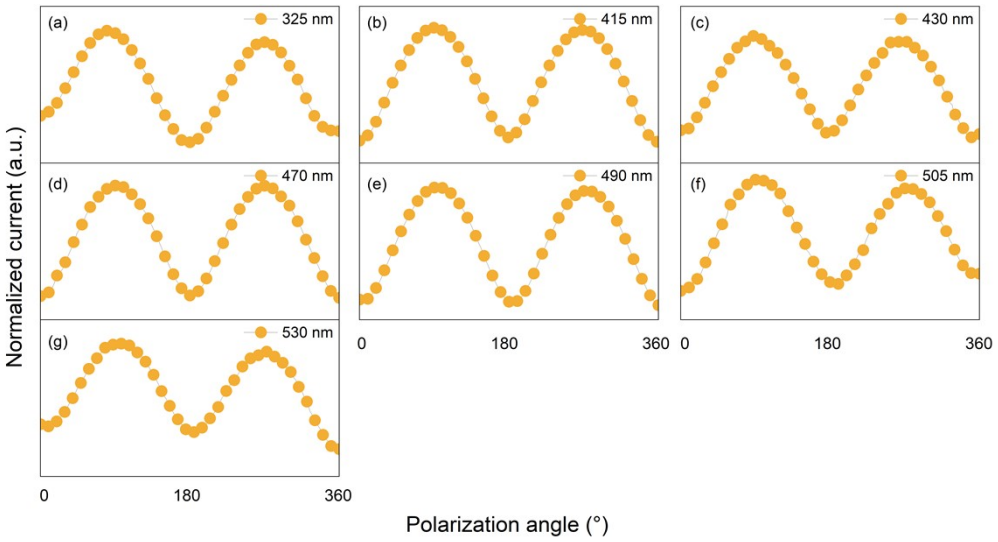

Fig. S4. Angle-dependent photocurrent of 2TM-1 measured at different wavelengths.

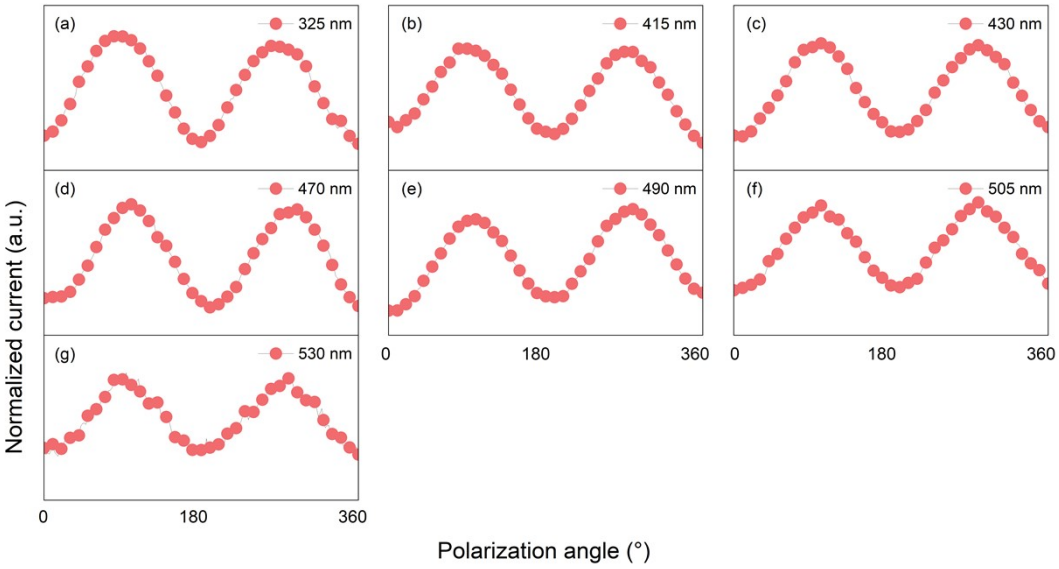

Fig. S5. Angle-dependent photocurrent of 2TM-2 measured at different wavelengths.

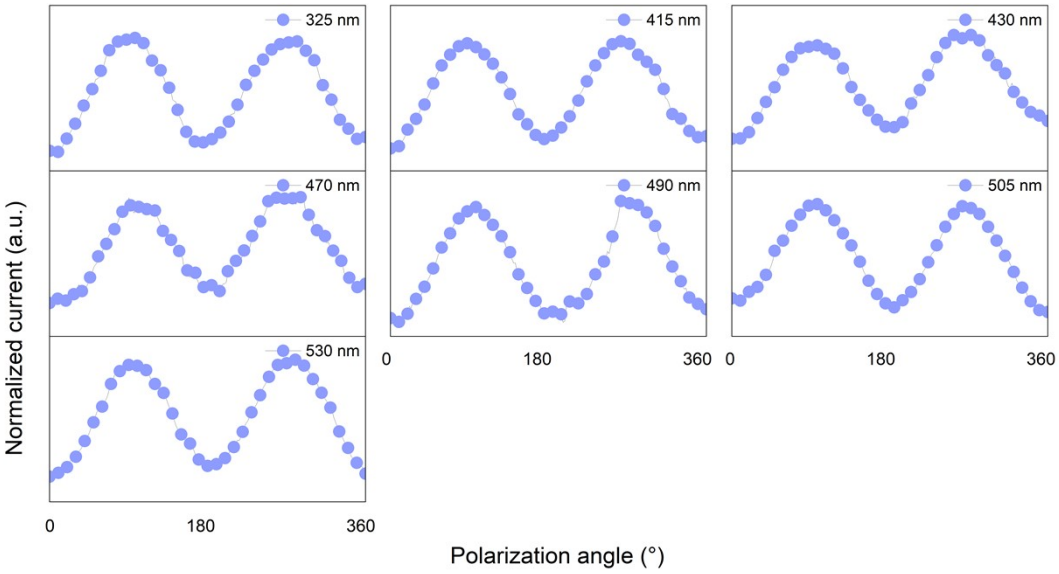

Fig. S6. Angle-dependent photocurrent of 2TM-3 measured at different wavelengths.

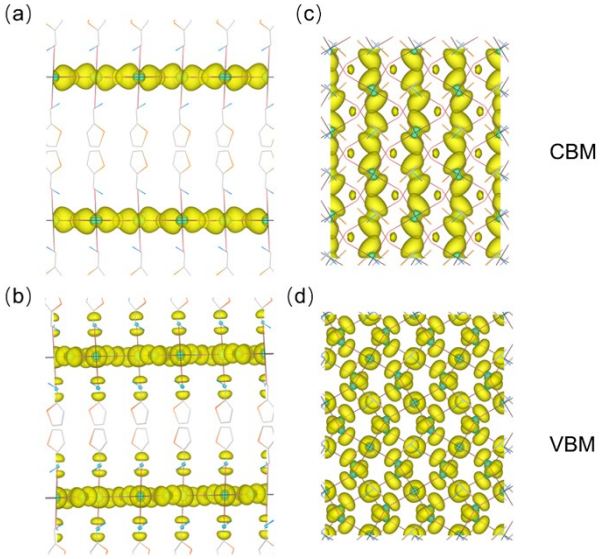

Fig. S7. Calculated CBM and VBM partial charge densities of 2TM-1.

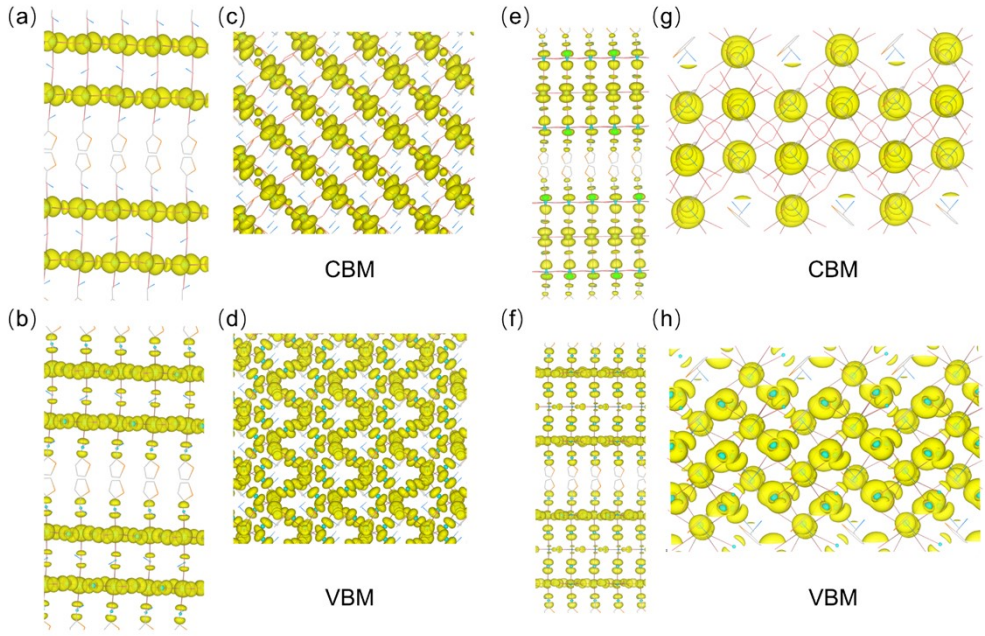

Fig. S8. Calculated CBM and VBM partial charge densities of (a-d) 2TM-2 and (e-f) 2TM-3.

Reference

[1] a) J. P. Perdew, K. Burke, M. Ernzerhof, *Phys. Rev. Lett.* **1996**, 77, 3865; b) H. J. Monkhorst, J. D. Pack, *Phys. Rev. B* **1976**, 13, 5188; c) J. Paier, M. Marsman, K. Hummer, G. Kresse, I. C. Gerber, J. G. Angyan, *J. Chem. Phys.* **2006**, 124, 154709; d) V. Wang, N. Xu, J. C. Liu, G. Tang, W. T. Geng, *Comput. Phys. Commun.* **2021**, 267, 19, 108033.

[2] a) H. Yang, L. Pan, X. Wang, H. X. Deng, M. Zhong, Z. Zhou, Z. Lou, G. Shen, Z. Wei, *Adv. Funct. Mater.* **2019**, 29, 1904416; b) Z. Zhou, M. Long, L. Pan, X. Wang, M. Zhong, M. Blei, J. Wang, J. Fang, S. Tongay, W. Hu, J. Li, Z. Wei, *ACS Nano* **2018**, 12, 12416.